

NASA Technical Memorandum 88259

Airborne Astronomy Program
Medium Altitude Missions Branch
Preprint Series 053

(NASA-TM-88259) INFRARED REFLECTION NEBULAE
IN ORION MOLECULAR CLOUD 2 (NASA) 46 p
CSSL 03A

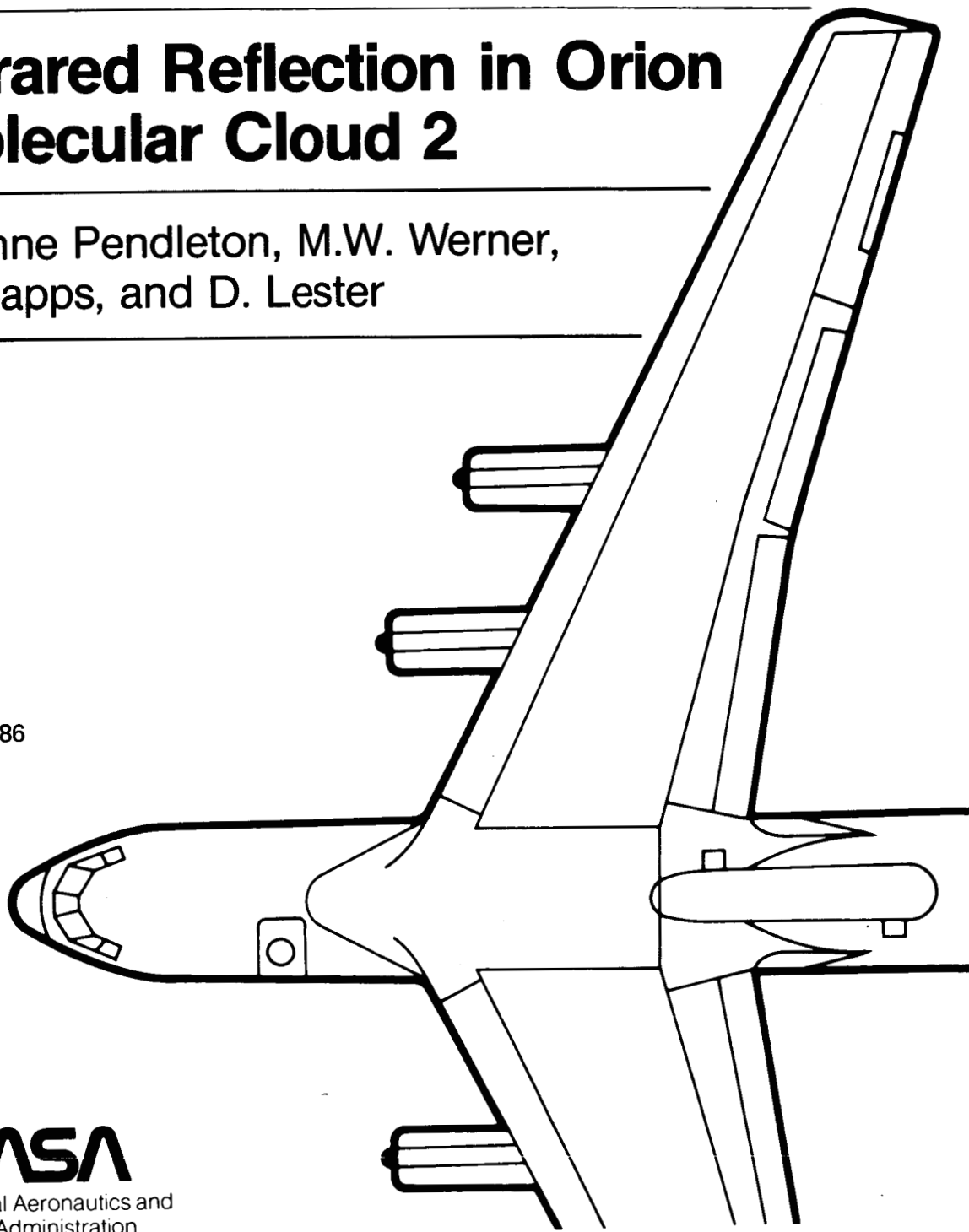
N87-13363

Unclas
G3/89 44663

Infrared Reflection in Orion Molecular Cloud 2

Yvonne Pendleton, M.W. Werner,
R. Capps, and D. Lester

June 1986



NASA
National Aeronautics and
Space Administration

Infrared Reflection in Orion Molecular Cloud 2

Yvonne Pendleton, Ames Research Center, Moffett Field, California

University of California, Santa Cruz, California

M. W. Werner, Ames Research Center, Moffett Field, California

R. Capps, University of Hawaii, Honolulu, Hawaii

D. Lester, University of Texas, Austin, Texas

June 1986

NASA

National Aeronautics and
Space Administration

Ames Research Center
Moffett Field, California 94035

INFRARED REFLECTION NEBULAE IN ORION MOLECULAR CLOUD 2

Yvonne Pendleton^{1,4,5}

M. W. Werner^{1,4}

R. Capps^{2,4}

D. Lester³

Received by the Astrophysical Journal March 11, 1986

¹ NASA Ames Research Center, Moffett Field, CA

² University of Hawaii, Honolulu, HI

³ University of Texas, Austin, TX

⁴ Visiting Astronomer at the Infrared Telescope Facility which is operated by the University of Hawaii under contract from the National Aeronautics and Space Administration.

⁵ University of California, Santa Cruz, CA

Abstract

New observations of Orion Molecular Cloud-2 have been made from 1-100 μ m using the NASA Infrared Telescope Facility and the Kuiper Airborne Observatory. An extensive program of polarimetry, photometry and spectrophotometry has shown that the extended emission regions associated with two of the previously known near infrared sources, IRS1 and IRS4, are infrared reflection nebulae, and that the compact sources IRS1 and IRS4 are the main luminosity sources in the cloud. The constraints from the far infrared observations and an analysis of the scattered light from the IRS1 nebula show that OMC-2/IRS1 can be characterized by $L \leq 500L_{\odot}$ and $T \sim 1000K$. The near infrared (1-5) μ m albedo of the grains in the IRS1 nebula is greater than 0.08.

I. INTRODUCTION

Infrared polarimetry can be an effective tool in an investigation of dust embedded prestellar objects and their surrounding medium. Polarimetry has shown in many instances that the extended near infrared emission in regions of star formation is scattered light, since it shows high polarization that can be produced only by scattering (Tokunaga et al,1981; Werner, Dinerstein, and Capps, 1983; Joyce and Simon,1986). In regions that are polarized by scattering, the orientations of the electric vectors clearly identify the luminosity sources. The scattering provides a second look at the illuminating object, through the reflected light, which can be complementary to direct line of sight observations of the source.

We have used infrared polarimetry to probe the infrared cluster in Orion Molecular Cloud-2 (OMC-2). OMC-2 is a 2'.5 x 3'.0 region of infrared and molecular emission located about 12' northeast of the Trapezium. Gatley et al (1974) have shown that, at 2.2 μ m, OMC-2 contains five point sources plus extended emission. We use their nomenclature (IRS1, IRS2, etc.) to identify the point sources. The redness of these objects, the absence of optical counterparts, and their association with molecular emission peaks (Batra et al,1983, Kutner et al, 1976) suggest that this is a region of current star formation. Thronson et al (1978) have measured a total luminosity for OMC-2 in the far infrared of 2100 L_{\odot} into a 3.5' beam. The absence of ionizing radiation and the low luminosity imply that if stars are forming in OMC-2, they are less massive than those forming in the core of OMC-1. In this paper we present new observations of OMC-2 which include photometry, spectrophotometry and polarimetry in the 1-30 μ m region as well as 50 μ m and 100 μ m photometric maps. We have determined that the extended emission in the region of OMC-2/IRS1 is a particularly good example of an

infrared reflection nebula. We have also identified, in the near infrared, a second region of high polarization and a previously unresolved double source structure in OMC2-IRS4. The far infrared measurements have allowed us to identify OMC-2/IRS1 and OMC-2/IRS4 as the primary luminosity sources within the cluster, to determine their luminosities, and to infer the dust optical depths and grain temperatures. The total luminosity inferred from the far infrared measurements provides an important additional constraint to the interpretation of the near infrared data; the near and far infrared observations together set new constraints on the properties of the embedded sources in this region.

II OBSERVATIONS

A. NEAR INFRARED

The 1-30 μm observations were made at the NASA Infrared Telescope Facility from 1982 October to 1984 December, using the facility instruments. Broadband photometry, one dimensional scans and/or comprehensive mapping were done at 1.25 μ ($\Delta\lambda=0.3$), 1.65 μ ($\Delta\lambda=0.35$), 2.2 μ ($\Delta\lambda=0.42$), 3.1 μ ($\Delta\lambda=0.1$), 3.8 μ ($\Delta\lambda=0.67$), and 4.8 μ ($\Delta\lambda=0.57$), with either a 6" or 4" beam, using the IRTF InSb system. The chopper spacing was between 35" and 45" north-south for the IRS1 measurements and 60" east-west for the IRS4 region. Spectra were obtained in the $2.8 \leq \lambda \leq 3.7 \mu\text{m}$ range with resolution of 2%. The 8.7 μ ($\Delta\lambda=1.2$), 9.7 μ ($\Delta\lambda=1.2$), 10.3 μ ($\Delta\lambda=5.2$), 12.5 μ ($\Delta\lambda=1.2$), 20 μ ($\Delta\lambda=9$), and 30 μ ($\Delta\lambda=8$) photometry was done with the IRTF Ge:Ga bolometer, using 4" and 8" beams. The chopper spacing for the 9-30 μm observations was 30" east-west. Absolute fluxes were determined by using standard calibration stars with calibration uncertainties of $\leq 10\%$ in the 1-5 μm range and $\leq 25\%$ in the 9-30 μm range.

Polarization measurements were made in the 2.2 μm and 3.8 μm broad band filters using a rotating wire grid as described in Werner et al, (1983). The polarization results were corrected for instrumental polarization (typically $\leq 2\%$) by subtracting the net polarization values measured for several intrinsically unpolarized stars. Absolute position angles were determined by reference to BN for which the position angle is known to be 117° measured east from north (Dyck and Lonsdale, 1979, and references therein).

We determined the positions of IRS1 and of both components of IRS4 relative to that of IRS3 which is known to be located at $\alpha(1950) = 5^{\text{h}}32^{\text{m}}59^{\text{s}}.1 \pm 0^{\text{s}}.1$, $\delta(1950) = -5^\circ 12' 10" \pm 1"$ (Gatley et al, 1974). Positions and offsets for

IRS1 and IRS4 relative to IRS3 are given in Table 1.

B. Far Infrared

Photometric maps were made with a 30" FWHM beam at 50 μm ($\Delta\lambda=25\mu\text{m}$) and 100 μm ($\Delta\lambda=50\mu\text{m}$) in February 1984 from the Kuiper Airborne Observatory at an altitude of 12.5km. The University of Texas six channel photometer (Wilking et al,1984) mounted at the Cassegrain focus of the KAO 91-cm telescope allowed measurements in both passbands to be made at each of three positions on the sky simultaneously. The instrumentation is similar to that described by Harvey (1979). The maps were made by offsetting in the KAO focal plane from a guide star located at $\alpha(1950)= 5^{\text{h}}33^{\text{m}}06.4^{\text{s}}$, $\delta(1950) = -5^{\circ}08'14''$. The positional uncertainties are $\pm 5''$. Position steps of 20".3 were taken in the north-south direction and 10".2 in the east-west direction until an area of 2'.5 x 3'.0 was covered;the area mapped is outlined by the dashed line in Figure 1. The chopper spacing was 5'in azimuth, which was close to east-west for these observations. The far infrared observations were calibrated relative to S140-IR (Harvey, Wilking,and Joy,1984). The calibration uncertainty is -20%.

III RESULTS

A. FAR INFRARED MAPS

Figures 1 and 2 show the flux contour maps at 50 and 100 μm , respectively. The near infrared source positions for IRS1, IRS2, IRS3, and IRS4, which we determined from 2.2 μm photometry, and the position of IRS5 determined by Gatley et al (1974), are indicated on these maps. The 50 μm map shows two peaks, one coincident with the position of IRS4 and a second, less pronounced peak coincident with the position of IRS1, as well as a slight amount of emission extended in the direction of IRS3. The 100 μm map is dominated by the peak at IRS4 and shows emission extended toward IRS1 which does not appear as a distinct peak. The spatial distribution and extent of the extended emission seen at 100 μm is similar to that seen at 2.2 μm by Gatley et al (1974), as shown in Figure 2.

The results of the infrared photometry and polarimetry are given in Table 2. The 50 μm flux densities into the 30" beam are 530 Jy for IRS4 and 185 Jy for IRS1. The former result is consistent with the flux density of 570 Jy measured at 61 μm into a 18"x28" beam that included IRS4 and IRS1 by Thronson et al (1978). The far infrared maps show that the region around IRS3 does not emit strongly at 50 μm so that the Thronson et al (1978) measurement is dominated by flux from IRS4. Color temperatures derived from the 50 and 100 μm data are between 35 and 50K in both the IRS1 and IRS4 regions. Assuming that the emissivity falls as λ^{-1} , grain temperatures for these areas are between 30 and 40K. Optical depths at 50 and 100 μm were derived from the grain temperature and the observed flux and show that both the IRS1 and IRS4 regions are optically thin. The peak optical depth at 100 μm towards IRS1 is $\tau_{100}=0.02$, which implies an average value for the visual extinction over the

-30" beam of $A_V \sim 15$, assuming $\tau_{UV}/\tau_{125} = 2000$ (Whitcomb et al, 1981) and an interstellar extinction law based on the results of Savage and Mathis (1979).

We measure a total flux of 5300 Jy at 100 μm and 715 Jy at 50 μm for the 2.'5 x 1.'8 area within the lowest contour on Figure 2. This implies a 40-150 μm luminosity of 900 L_\odot for this area, assuming a distance of 500 pc. This far exceeds the near infrared (1-20 μm) luminosity of $\sim 100 L_\odot$. IRS1 and IRS4 coincide with peaks in both 50 μm brightness and far infrared color temperature. Therefore, we conclude that IRS1 and IRS4 are the primary luminosity sources in OMC-2, and that the far infrared radiation is thermal emission from dust heated by these sources. The integrated flux into a 30" beam at the peak positions is 130 L_\odot for IRS1 and 400 L_\odot for IRS4. Thus, much of the luminosity of these sources is reradiated by the extended dust cloud. Our luminosity determination agrees satisfactorily with that of Thronson et al (1978), who measured 2100 L_\odot into a 3.'5 beam centered on OMC-2, using a $\sim 9'$ chopper throw.

B. Near Infrared

The photometry and polarimetry results are presented in Table 2. The near infrared photometric results agree with those of Gatley et al (1974). New observations of OMC-2/IRS2 are presented in Table 2, although they will not be discussed in the text.

1. IRS1

We mapped the extended emission in the region between IRS1 and IRS3 at 2.2 and 3.8 μm as shown in Figures 3 and 4 and also found the emission to be highly polarized at both wavelengths (up to 31% at 3.8 μm). The contours in Figures 3 and 4 are logarithmic to emphasize the low surface brightness

extended emission between the infrared peaks. The length of the dark lines in Figures 3 and 4 indicates the percent polarization, P , while the orientation of the dark lines displays the position angle of the maximum electric vector. The high polarization values of $6\% \leq P \leq 23$ at $2.2\mu\text{m}$ and $13\% \leq P \leq 31$ at $3.8\mu\text{m}$ suggests that scattering is responsible (Werner, Dinerstein, and Capps, 1983). The orientation of the electric vectors implies that IRS1 is illuminating the grains. Surface brightness measurements, shown in Figure 5, along a NE line extending radially outward from IRS1 through the nebula show that the nebula is fairly uniform in brightness and color, and that the color is significantly bluer than that of IRS1. All points in the nebula appear brighter than IRS1 at the shortest wavelengths, showing that there is localized extinction along our direct line of sight to IRS1. The $(1.25/4.8)\mu\text{m}$ color temperature in the nebula is $\geq 1000\text{K}$, too high to be attributable to thermal emission. Near infrared continuum emission with color temperature in this range has been seen in visual reflection nebulae by Sellgren, Werner, and Dinerstein (1983), where it is associated with ultraviolet radiation and the $3.3\mu\text{m}$ emission feature. Since neither of these appears to be present in OMC-2, we feel that it is unlikely that the (presumably non-equilibrium) processes producing the emission in visual reflection nebulae are occurring in OMC-2. Based on the high near infrared color temperature and the high polarization, we therefore assume below that all of the $1-5\mu\text{m}$ radiation from the nebula is scattered light even though we have polarimetry only at 2.2 and $3.8\mu\text{m}$.

The $3.05\mu\text{m}$ absorption feature, attributed to ice, appears in the spectra of all points observed in the nebula as well as in the spectrum of IRS1. The CVF spectra of IRS1 and a point in the nebula are shown in Figure 5b. Along the line of sight to IRS 1, the $3.05\mu\text{m}$ feature has an optical depth of $\tau=2$ and along the line of sight to a point in the nebula located $20''$

from IRS1 $\tau=1.2$. The optical depths were derived by assuming a continuum level between 2.2 and 3.8 μm from the energy distributions shown in Figure 5. The continuum level was taken to be the intrinsic intensity, I_{int} , while the intensity measured in the depth of the ice band at 3.05 μm was taken to be the observed intensity, I_{obs} . Optical depths were derived from the relationship

$$I_{\text{obs}}/I_{\text{int}}=e^{-\tau_{3.05}}.$$

The higher optical depth towards IRS1 supports our assertion that a large amount of localized extinction exist towards IRS1. The 3.3 μm emission feature which appears in the spectra of visual reflection nebulae (Sellgren et al) is not present in the spectrum of either IRS1 or the nebula.

2. IRS3

Polarization measurements, given in Table 2, show that IRS-3 is weakly polarized at 2.2 and 3.8 μm . The 1-20 μm energy distribution for IRS-3 is shown in Figure 6. The total 1-20 μm luminosity is $50L_{\odot}$. Our results show that IRS-3 is a point source which peaks around 5 μm . The far-IR data suggest that it is not a major luminosity source in the cloud.

3. IRS4

At 3.8 μm IRS4 was resolved with a 4" beam into two components, as shown in the 3.8 μm map in Figure 7. The components are separated by 4" in the north-south direction and will be referred to as IRS4-N and IRS4-S hereafter. IRS4-N is highly polarized at 3.8 μm . A series of N-S scans through IRS4 shown in Figure 8 reveals the interesting nature of IRS4-N. It is comparably bright to IRS4-S at 3.8 μm and 4.8 μm , but is not seen as a discrete feature at either shorter or longer wavelengths until 20 μm , where it appears brighter than IRS4-S. The importance of IRS4-N at the longer

wavelengths is further demonstrated by 30 μ m observations with 4" and 8" apertures, which show that most of the flux from IRS4 arises from a source smaller than 4" and centered on IRS4-N. Comparison observations made with a point source, α Ori, and an extended object, BN, demonstrated that the flux from IRS4 originates from a compact region. For this reason, we assume that the 50 μ m and 100 μ m radiation from IRS4 is associated with IRS4-N, which would then be the dominant luminosity source in the cluster. The 0.94 μ m photograph published by Cohen and Frogel (1974) shows two components in the IRS4 region. By comparison of their photograph to the starfield visible in the guider at the IRTF we determined that the northernmost component seen by those investigators coincides with the source we call IRS4-S; IRS4-N has not previously been identified.

IV DISCUSSION

A. IRS1 and the Adjacent Reflection Nebula

The classical method of dereddening the directly observed energy distribution fails badly in the case of OMC-2/IRS1 because we do not know what to assume for the wavelength dependence of extinction in this region and because even with a 4" aperture the flux observed directly from the position of IRS1 includes contributions due to scattered light at wavelengths shorter than about $4\mu\text{m}$. We feel the simple arguments presented below demonstrate the usefulness of the scattered light as an alternate means of determining the nature of embedded objects. A similar approach has been used by Lenzen et al (1984) in their analysis of Cep A.

a. Luminosity of IRS1

The results of Thronson et al show that the total luminosity of OMC-2 is no greater than $\sim 2100L_{\odot}$. Assuming that IRS1 and IRS4 make up the total luminosity, an estimate can be made of the luminosity of each. We scale the total luminosity according to the integrated flux into a 30" beam at the peak positions. Since L_{IRS4} is approximately four times as bright as IRS1, we assume that $L_{\text{IRS1}} \leq 500L_{\odot}$. Our measurement of the total luminosity of OMC-2 is $\sim 900L_{\odot}$. Because the results of Thronson et al show that the diffuse emission from outside the area mapped by us contributes significantly to the overall luminosity of the cloud, we feel that $500L_{\odot}$ is a conservative upper limit for the luminosity of IRS1.

b. Temperature of IRS1

The far infrared results which show that IRS1 is a primary luminosity source fit well with the near infrared polarimetry at 2.2 and 3.8 μ m which clearly identifies IRS1 as the illuminating source for the adjacent reflection nebula. We can use this circumstance to calculate the near infrared blackbody temperature of IRS1 by assuming that all of the 1-5 μ m radiation from the nebula is scattered light, and that IRS1 is the sole illuminating source for the scattering grains. The scattered light from the nebula, together with the luminosity determined from the far infrared observations, then provide a constraint on the temperature of IRS1. This analysis is approximate, but instructive. A more complete picture will result from detailed modelling of this region.

We have assumed that the nebular geometry is such that internal extinction and multiple scattering within the nebula can be neglected, that there is no reddening along our line of sight to the nebula, and that IRS1 can be described as a blackbody of temperature T. The neglect of internal extinction is consistent with the uniformity of surface brightness and color of the nebula (Figure 5). Knowing the luminosity of IRS1 from the far infrared observations, the flux which illuminates the nebula at each wavelength can be determined for any value of T, and the scattering probability in the 1-5 μ m range can be calculated. The scattering probability, $P(\lambda)$, is defined as the total flux scattered from a particular line of sight through the nebula, $F_{\lambda}(\text{neb})$, divided by the illuminating flux reaching the grains along that line of sight:

$$P(\lambda) = \frac{F_{\lambda}(\text{neb}) \times 4\pi R^2}{L_{*} \langle F(\lambda, T) + \sigma T^4 \rangle \langle \Omega + 4\pi \rangle}$$

where $F_{\lambda}(\text{neb})$ is the nebular flux observed at wavelength λ , R is the distance to the source, L_{*} is the luminosity of the star, $F(\lambda, T)$ is the flux emitted from a blackbody of temperature T at wavelength λ , σ is the Stephan-Boltzmann constant, and Ω is the solid angle subtended at the star by the portion of the nebula included in the beam. We analyze a position 14"E and 14"N of IRS1, where the nebula was measured with a 6" beam, so $\Omega \sim 0.3$ sr. We have taken L to be $500L_{\odot}$ and $R=500\text{pc}$.

Figure 9 displays $P(\lambda)$ for assumed temperatures of 850 and 1200K for IRS1. For $T \leq 850\text{K}$, $P(\lambda)$ approaches unity at the shortest wavelengths. Since the probability cannot exceed unity, $T \leq 850\text{K}$ is not reasonable. At $T \geq 1200\text{K}$, $P(\lambda)$ increases with wavelength at the longer wavelengths which is inconsistent with general scattering theory for small particles with radius less than or equal to the wavelength. Applying the constraints on $P(\lambda)$ that it not exceed unity at any wavelength and that it decreases with increasing wavelength, this simplified model of IRS1 and the adjacent nebula suggests that IRS1 is at a temperature of approximately 1000K. We note that this conclusion is based on the wavelength dependence as well as the absolute value of $P(\lambda)$. Although extinction within the nebula or along the line of sight could affect the results somewhat, large amounts of extinction would be required to produce significant changes in the color of the scattered light and thus in the range of plausible temperatures. However, introducing more than a few magnitudes of extinction results in $P(\lambda)$ coming implausibly near unity. Thus to the extent that the near infrared energy distribution of the illuminating radiation from IRS1 can be described by a single blackbody temperature, we feel that the temperature must be close to 1000K. The amount of extinction implied by matching the assumed physical properties of IRS1 ($L=500L_{\odot}$, $T=1000\text{K}$) with our direct near infrared observations of IRS1 is ~ 3.5

magnitudes at $4.8\mu\text{m}$; this wavelength is chosen as being least affected by scattering or thermal emission. Assuming $\tau(\lambda)$ varies as $\lambda^{-1.45}$ (Becklin et al, 1978) gives $A_V \sim 75$ along the line of sight to IRS1; alternatively, the extinction law derived by Rieke and Lebofsky (1985) suggest $A_V \sim 85-90$. This estimate of the extinction refers only to the direct line of sight to the illuminating object, IRS1, which is known from the scattered light data to pass through localized extinction. Thus, the estimate derived here can be reconciled with the lower value, $A_V \sim 15$ derived from the far infrared optical depth averaged over a $30''$ field of view including IRS1.

Because IRS1 is an infrared source, the far infrared emitting grains in the IRS1 nebula must be heated at infrared wavelengths. A comparison with the visual reflection nebula NGC7023 studied by Whitcomb et al (1981) demonstrates that this is plausible. In NGC 7023, the heating flux (emitted primarily at $\sim 2000\text{\AA}$) received by a grain at a projected distance of 0.2 pc from the central star is $3.5\text{E-}7 \text{ Wcm}^{-2}$. In the OMC-2/IRS1 nebula the same amount of flux is received by a grain located $30''$ from IRS1, which corresponds to a projected distance of 0.07 pc. The dust grain temperatures at the aforementioned positions are 55K in the NGC 7023 nebula and 29K in the OMC-2/IRS1 nebula even though the grains receive the same amount of flux. The lower dust temperature in the IRS1 nebula can be understood qualitatively if the grains are heated at infrared wavelengths since grains absorb less efficiently in the infrared than in the UV. The same result is obtained even if half of the $100\mu\text{m}$ flux at the position $30''$ from IRS1 is attributed to material elsewhere along the line of sight heated by IRS4.

To summarize, our data suggest that IRS1 is an object with $T=1000\text{K}$ and $L \sim 500L_{\odot}$. Our direct view of it is obscured by localized extinction, while the grains in the nebula are illuminated by IRS1 with little intervening

extinction. Several possibilities exist as to the nature of IRS1. It could be a fairly mature star embedded in a circumstellar shell which radiates at 1000K. It is perhaps more satisfying to assume that IRS1 is a younger object, so that 1000K is the temperature of the collapsing envelope of a protostar. Under this assumption, comparison with published protostellar tracks (Larson, 1972) show that the inferred luminosity and temperature are characteristic of a $3-5M_{\odot}$ object about 10^6 years after the onset of collapse.

c. Grain Properties

For $T=1000K$, we find $P=0.05$ as an average value between 1 and $5\mu m$ (Figure 9). The neglect of extinction along the scattering path, and the fact that L may be $<500L_{\odot}$ for IRS1 underestimate P . The scattering probability is related to the grain albedo ω as

$$P = \tau(\text{neb}) \times \omega$$

where $\tau(\text{neb})$ is the optical depth to the illuminating radiation along a ray through the region of the nebula within the observing beam. Because $\tau(\text{neb}) \leq 1$, we have $\omega \geq P$. A more straightforward way to estimate ω , which is independent of specific assumptions about the illuminating source, is to calculate the albedo by comparing the intensity of the scattered $1-5\mu m$ light and the intensity of the far infrared radiation. The similarity of the $100\mu m$ and $2.2\mu m$ dust distribution and the fact that IRS1 is heating grains at near infrared wavelengths imply that the dust which scatters light in the near infrared is also radiating at $100\mu m$, and that it is heated by the near infrared radiation which it absorbs rather than scatters. Because

$$\omega = \sigma(\text{scat}) / \langle \sigma(\text{scat}) + \sigma(\text{abs}) \rangle$$

where $\sigma(\text{scat})$ is the scattering cross-section and $\sigma(\text{abs})$ is the absorbing cross-section, we can estimate the near infrared albedo of the dust in the IRS1

nebula by taking $\sigma(\text{scat})$ proportional to $B(\text{scat})$, the surface brightness of the 1-5 μm flux and $\sigma(\text{abs})$ proportional to $B(\text{abs})$, the luminosity integrated over wavelength from the 50 and 100 μm measurements. Thus,

$$\omega = B(\text{scat}) / \langle B(\text{scat}) + B(\text{abs}) \rangle.$$

The point in the nebula used for this calculation is located 20"NE from IRS1. $B(\text{abs}) = 5.5\text{E-}8 \text{ Wcm}^{-2}\text{sr}^{-1}$ and $B(\text{scat}) = 4.6\text{E-}9 \text{ Wcm}^{-2}\text{sr}^{-1}$ at this point. We find $\omega = 0.08$ as an average value from 1-5 μm in this fashion. The 100 μm map (Figure 2) shows that grains heated by IRS4 may contribute to the flux from the IRS1/nebula region. If so, this calculation underestimates the albedo. We also have neglected the effects of multiple scattering and internal extinction, both of which would also serve to make the albedo, as calculated above, less than the true albedo. Therefore, 0.08 should be considered a lower limit to the true grain albedo. A comparison of our result for grain albedos in the near infrared to standard grain models (Draine and Lee, 1984) reveals that a mixture of graphite and silicate grains in a Mathis, Rumpl, Nordsieck size distribution (1977) could have the near infrared albedo ≥ 0.08 required by the data.

d. Polarimetry and Spectrophotometry

The percent polarization increases with distance from the source at both 2.2 and 3.8 μm . Although the polarization measured near the source will be diluted by the variation of scattering angles across the beam, this effect can account for no more than ten percent of the increase in polarization we observe. Another possibility is that the effect is due to the geometry of the IRS1 nebula. If the scattering angle is closer to 90° at larger distances from the source, it may account for the higher polarization seen at those points. We note that the polarization is larger at 3.8 μm than at 2.2 μm , a

trend that increases close to the source. This may imply that the effects of multiple scattering must be included in any comprehensive model of this region. The wavelength and spatial variation of polarization will be investigated through further modeling.

The absence of the 3.3 μm emission feature which appears in the spectra of visual reflection nebulae indicates that the mechanism which excites this feature is not present in OMC-2. This is consistent with the idea put forth by Sellgren (1983) that the absorption of ultraviolet photons by small grains or large molecules produces the 3.3 μm feature by a non-equilibrium process. There are no UV photons available to produce this feature in the IRS1 nebula because the illuminating star is an infrared source.

The 3.1 μm ice band absorption feature appears in the spectra of both the illuminating source and the reflection nebula. It is not clear whether the feature originates in a dust shell surrounding IRS1, in the nebula, or in line-of-sight material. A correlation has been observed between the depth of the 3.1 μm absorption feature and high polarization in star formation regions (Joyce and Simon, 1982 and 1986). These authors suggest that metallic oxide grain cores surrounded by icy mantles are responsible for this correlation. In their model the ice absorption is produced by the mantles while the polarization is a result of grain alignment in a magnetic field, which may be enhanced by the paramagnetic properties of the mantle (Duley, 1978). This model may apply to objects such as the BN object where dichroic absorption is responsible for the polarization. In the case of OMC-2/IRS1, however, our observations which show both high polarization due to scattering and an ice band in the spectrum of the nebula suggest that a geometrical explanation for this correlation is likely. Consider a source

with the general character of OMC2/IRS1 observed from two angles (Figure 10). An observer with an obscured view of the star sees high polarization and a deep ice band. This corresponds to our view of OMC-2/IRS1. An observer looking in from an orthogonal direction will see the central object more clearly and much lower polarization because of symmetry and because a much smaller fraction of the light is scattered. The observer will also see a weaker ice band (see Figure 10). If this geometrical effect is in fact the correct explanation for the Joyce-Simon correlation, it implies that the ice band may not be present in the intrinsic spectrum of the source which illuminates the reflection nebula in OMC2 or in similar objects. It is interesting to examine what the OMC-2/IRS1 region would look like if it were at a distance such that it could not be spatially resolved. We calculate the percent polarization, averaged over the IRS1 nebula, to be 13% at $2.2\mu\text{m}$ while the optical depth of the ice band is $\tau=1.2$. The source would then appear similar to those objects cited by Joyce and Simon as having deep ice bands and high polarization. Note that other reflection nebulae show ice band absorption (Cep A, Lenzen et al, 1984; NGC 6334, Simon et al, 1985). These objects, like OMC2/IRS1, have both deep ice bands and high polarization. In each case it is clear that the principal polarization mechanism is scattering rather than dichroic absorption.

B. The IRS3 Region

Unlike the cases of IRS1 and IRS4, the flux from IRS3 peaks in the near infrared. The absence of appreciable far infrared emission suggests that IRS3 is not a prime luminosity source within the cloud and indicates that our view of IRS3 is not influenced by large amounts of extinction local to the source. The weak ice band observed toward IRS3 is consistent with this picture. The absence of associated strong far infrared emission makes OMC-

2/IRS3 rather unusual among embedded infrared sources; perhaps complex geometries and dust distributions like that sketched in Figure 10 are common so that only in rare cases does one get a direct view of the central star or protostar. One could then refer to OMC-2/IRS3 as a "naked protostar". An alternative possibility is that IRS3 is a background object viewed through the cloud.

C. The IRS4 Region

The two components of IRS4 exhibit unusual phenomenology (Figure 8). The northern component, IRS4-N, is comparably bright to the southern component, IRS4-S, at $3.8\mu\text{m}$ and $4.8\mu\text{m}$, but is not seen at longer wavelengths until $20\mu\text{m}$. From the $3.8\mu\text{m}$ polarimetry IRS4-N appears to be an infrared reflection nebula which is illuminated by IRS4-S. The absence of IRS4-N at $8.7, 9.7$ and $12.5\mu\text{m}$ is understandable under this picture, since scattering is less efficient at longer wavelengths. The continuity of the polarization with position shown in Figure 8b argues against the possibility that IRS4-N is a background source seen at 2.2 and $3.8\mu\text{m}$ through polarized foreground scattered light. However, at $20\mu\text{m}$ and $30\mu\text{m}$ IRS4-N is the dominant member of the pair and indeed the most luminous object in OMC2. Clearly, two phenomena, a luminous far infrared source and a near infrared reflection nebula, are both located along the line of sight to IRS4-N. It is logical to attribute these phenomena to a single object. One intriguing possibility is that the scattering at $3.8\mu\text{m}$ is due to an extended envelope or dust shell which surrounds IRS4-N and is illuminated at short wavelengths by IRS4-S. In detail we have found it difficult to make this model work, basically because IRS4-N is much redder than IRS4-S at $2.2\mu\text{m}$. The other possibility is that IRS4-N itself is responsible for illuminating a very compact, very local reflection nebula at short wavelengths. In this case, the orthogonality of the polarization

position angles to the direction toward IRS⁴-S is merely coincidental.
Further work, perhaps at very high spatial resolution, will be required to
improve our understanding of this peculiar pair of objects.

D. Comparison of Infrared and Visible Reflection Nebulae

Ultraviolet and visual observations of reflection nebulae such as NGC7023 and the Pleiades have been one of the main means of obtaining data on the properties of interstellar grains at these wavelengths (Witt et al,1982). Sellgren,Werner, and Dinerstein (1983) extended the data on this class of objects to longer wavelengths but found the infrared emission to be dominated by non-equilibrium processes the nature of which is still uncertain (Sellgren,1984;Sellgren ,1985). Thus classical visual reflection nebulae illuminated by early-type stars are not good sites for the study of the infrared properties of the bulk of the interstellar grains. It now appears that such information may be obtainable through the study of infrared reflection nebulae,such as OMC-2, which are illuminated by infrared sources. The brightness of the scattered infrared radiation can be quite high for present techniques, and the absence of ultraviolet radiation suppresses the non-equilibrium infrared emission seen in the visual nebulae. In subsequent papers, we will construct models of infrared reflection nebulae to determine the constraints which observations such as these place upon the properties of interstellar grains.

V. Conclusions

We have carried out an extensive program of polarization, photometry, and spectrophotometry of the OMC-2 cluster at infrared wavelengths from 1-100 μ m. We find that the point sources in the cluster are embedded in a complex and inhomogeneous distribution of dust clouds which strongly modify our view of them. The results highlight the prevalence of 1-5 μ m reflection nebulae in regions of star formation and the consequent importance of polarimetry as a probe of such regions. We have identified the OMC-2/IRS1 nebula as a particularly good example of an infrared reflection nebula that is well suited to further observational and theoretical study. In conclusion, our results show that:

1. The compact sources IRS1 and IRS4 are the main luminosity sources in the OMC2 region. IRS1 illuminates the grains in the adjacent reflection nebula, IRS4 has double source structure, and IRS3, the brightest object in the region at $\lambda=10\mu$ m, is not an important luminosity source.
2. The reflected light from IRS1 provides additional constraints on and information about the illuminating source that cannot be obtained through direct line of sight observations. The analysis of the scattered light and the constraints from the far infrared observations show that OMC-2/IRS1 can be characterized by $L \leq 500L_{\odot}$ and $T \approx 1000\text{K}$. If IRS1 is a protostar with $L \sim 500L_{\odot}$, and $T \sim 1000\text{K}$, then it corresponds to a $3-5M_{\odot}$ object at an age of $\sim 10^6$ years following the onset of collapse.
3. The near infrared (1-5) μ m albedo of the grains in the nebula is $\omega \geq 0.08$.

Acknowledgments

We thank Harriet Dinerstein, Paul Harvey, Marshall Joy, Charlie Kaminski, Kris Sellgren and Xander Tielens for assistance with the observations. We appreciate the support of the staffs of the Kuiper Airborne Observatory and the NASA Infrared Telescope Facility. We are grateful to Xander Tielens, Mike Castelaz, Lou Allamandola, Dick Miller, David Rank, and Peter Bodenheimer for helpful discussions. We also thank an anonymous referee for helpful comments and suggestions. The work at Ames has been supported by the Astrophysics Division of NASA, and the work at Texas by NASA grant NAG2-67.

REFERENCES

- Batrla, W., Wilson, T. L., Bastien, P., and Ruf, K., 1983, Astr. Ap., ~~128~~,
279.
- Becklin, E. E., Matthews, K., Neugebauer, G., and Willner, S. P., 1978,
Ap.J., ~~220~~, 831.
- Cohen, J. G. and Frogel, J., 1977, Ap.J., ~~211~~, 178.
- Draine, B. T., and Lee, H. M., 1984, Ap.J., ~~285~~, 89.
- Duley, W., W., 1978, Ap.J.(Letters), ~~219~~, L129.
- Dyck, H. M. and Lonsdale, C. J., 1979, A.J., ~~84~~, 1339.
- Gatley, I., Becklin, E. E., Matthews, K., Neugebauer, G., Penston, M. V.,
and Scoville, N., 1974, Ap.J.(Letters), ~~191~~, L121.
- Harvey, P., 1979, P.A.S.P., ~~91~~, 143.
- Harvey, P., Wilking, B., and Joy, M., 1984, Nature, ~~307~~, 441.
- Joyce, R. R. and Simon, T., 1982, Ap.J., ~~260~~, 604.

Joyce, R. R. and Simon, T., 1986, A.J., 91, 113.

Kutner, M. L., Evans II, N. J., and Tucker, K. D., 1976, Ap.J., 209, 452.

Larson, R.B., 1972, M.N.R.A.S., 157, 121.

Lenzen, R., Hodapp, K.-W., and Solf, J., 1984, Astr. Ap., 137, 202.

Mathis, J. S., Rumpl, W., and Nordsieck, K. H., 1977, Ap.J., 217, 425.

Rieke, G. and Lebofsky, M., 1985, Ap.J., 288, 618.

Savage, B. D. and Mathis, J. S., 1979, Ann. Rev. Astron. Astrophys., 17,
73.

Sellgren, K., Werner, M., and Dinerstein, H., 1983, Ap.J.(Letters),
271, L13.

Sellgren, K., 1984, Ap.J., 277, 623.

Sellgren, K., 1985, Ap.J., 299, 416.

Simon, T., Dyck, H. M., Wolstencroft, R. D., Joyce, R. R., Johnson, P. E.
and McLean, I. S., 1985, M.N.R.A.S., 212, 21P.

Thronson, H. A., Harper, D. A., Keene, J., Loewenstein, R. F., Moseley, H.
and Telesco, C. M., 1978, A. J., 83, 492.

Tokunaga, A. T., Lebofsky, M. J., Rieke, G. H., 1981, Astr. Ap., 99, 108.

Whitcomb, S. E., Gatley, I., Hildebrand, R. H., Keene, J., Sellgren, K.,
and Werner, M. W., 1981, Ap.J., 246, 416.

Wilking, B. A., Harvey, P. M., Lada, C. J., Joy, M., and Doering, C.
R., 1984, Ap.J., 279, 291.

Witt, A. N., Walker, G. A. H., Bohlin, R. C. and Stecher, T. P., 1982,
Ap.J., 261, 492.

Werner, M. W., Dinerstein, H. L., and Capps, R. W., 1983, Ap. J.(Letters),
265, L13.

Figure Captions

Figure 1 A $50\mu\text{m}$ map of the OMC-2 cluster made using a $30''$ beam on a $20.3''\times 10.2''$ grid. Contour levels are 0.1, 0.2, 0.3, 0.4, 0.5, 0.6, 0.7, 0.8 and 0.9 times the peak value of 530 Jy into a $30''$ beam. The $2.2\mu\text{m}$ positions of the near infrared peaks are designated by the + sign. The $2.5'\times 3.0'$ region mapped is outlined by the dashed contour.

Figure 2 A $100\mu\text{m}$ map of the OMC-2 cluster made using a $30''$ beam on a $20.3''\times 10.2''$ grid. Contour levels are 0.1, 0.2, 0.3, 0.4, 0.5, 0.6, 0.7, 0.8, and 0.9 times the peak value of 1620 Jy into a $30''$ beam. The $2.2\mu\text{m}$ positions of the near infrared peaks are designated by the + sign. The dashed line is the lowest contour of the $2.2\mu\text{m}$ flux measured by Gatley et al (1974).

Figure 3 A $2.2\mu\text{m}$ map of OMC-2/IRS1, IRS3, and the adjacent nebula made using a $6''$ beam on a $4''$ grid. Contour levels are 0.02, 0.03, 0.06, 0.13, 0.25, and 0.5 times the IRS3 peak value of 0.67 Jy into a $6''$ beam. Logarithmic contour levels were chosen to enhance the low level surface brightness of the map. The + sign signifies that polarization measured at that point was less than the 3σ level.

Figure 4 A $3.8\mu\text{m}$ map of OMC-2/IRS1, IRS3, and the adjacent nebula made using a $6''$ beam on a $4''$ grid. Contour levels are 0.008, 0.02, 0.03, 0.06, 0.13, 0.25, and 0.5 times the IRS3 peak value of 3.5 Jy into a $6''$ beam. Logarithmic contour levels were chosen to enhance the low level surface brightness of the map. The + sign signifies that the polarization measured at that point was less than the 3σ level.

Figure 5(a) 1.25 to 4.8 μ m broadband photometry energy distributions of IRS1 and three positions in the nebula measured along a radial line through the nebula at points 5"E,5"N; 8"E,8"N; and 14"E,14"N of IRS1.

(b) Circular Variable Filter (CVF) measurements of IRS1 and the 8"E,8"N point in the nebula made from $2.8 \leq \lambda(\mu\text{m}) \leq 3.7$ using a 6" beam.

Figure 6 1.25 to 20 μ m broadband energy distributions of IRS1 (4" beam) and IRS3 (6" beam).

Figure 7 A 3.8 μ m photometric map of IRS4N and IRS4S made using a 4" beam on a 2" grid. Contour levels are 0.1, 0.2, 0.3, 0.4, 0.5, 0.6, 0.7, 0.8, and 0.9 times the IRS4S peak value of 0.3 Jy into a 4" beam. Polarization measurements made with a 4" beam are shown on the map. The length of the dark line indicates the degree of polarization while the orientation of the dark line gives the position angle of the maximum electric vector. The + sign signifies that the polarization measured at that point was less than the 3σ level.

Figure 8 North-South photometric scans through IRS4 at $\lambda=2.2, 3.8, 4.8, 8.7, 9.7, 12.5,$ and 20 μ m, using a 4" beam, which show the relative flux of IRS4N and IRS4S. A polarization scan at 3.8 μ m is superposed on the 3.8 μ m flux scan. The scan was made by assuming a position angle of -90° at all points along this line, as suggested by Figure 7.

Figure 9 The near infrared scattering probability, P , as defined in the text is shown for intrinsic temperature values for IRS1 of 850K and 1200K.

Figure 10 A schematic diagram of the IRS1 nebula and the embedded protostar as seen from orthogonal directions.

Postal Addresses

Capps, R. W.

Institute for Astronomy

University of Hawaii

2680 Woodlawn Dr.

Honolulu, HI 96822

Lester, D, F.

Department of Astronomy

University of Texas

RLM Hall 15.308

Austin, TX 78712

Pendleton, Y. J.

NASA Ames Research Center

Mail Stop 245-6

Moffett Field, CA 94043

Werner, M.W.

NASA Ames Research Center

Mail Stop 245-6

Moffett Field, CA 94043

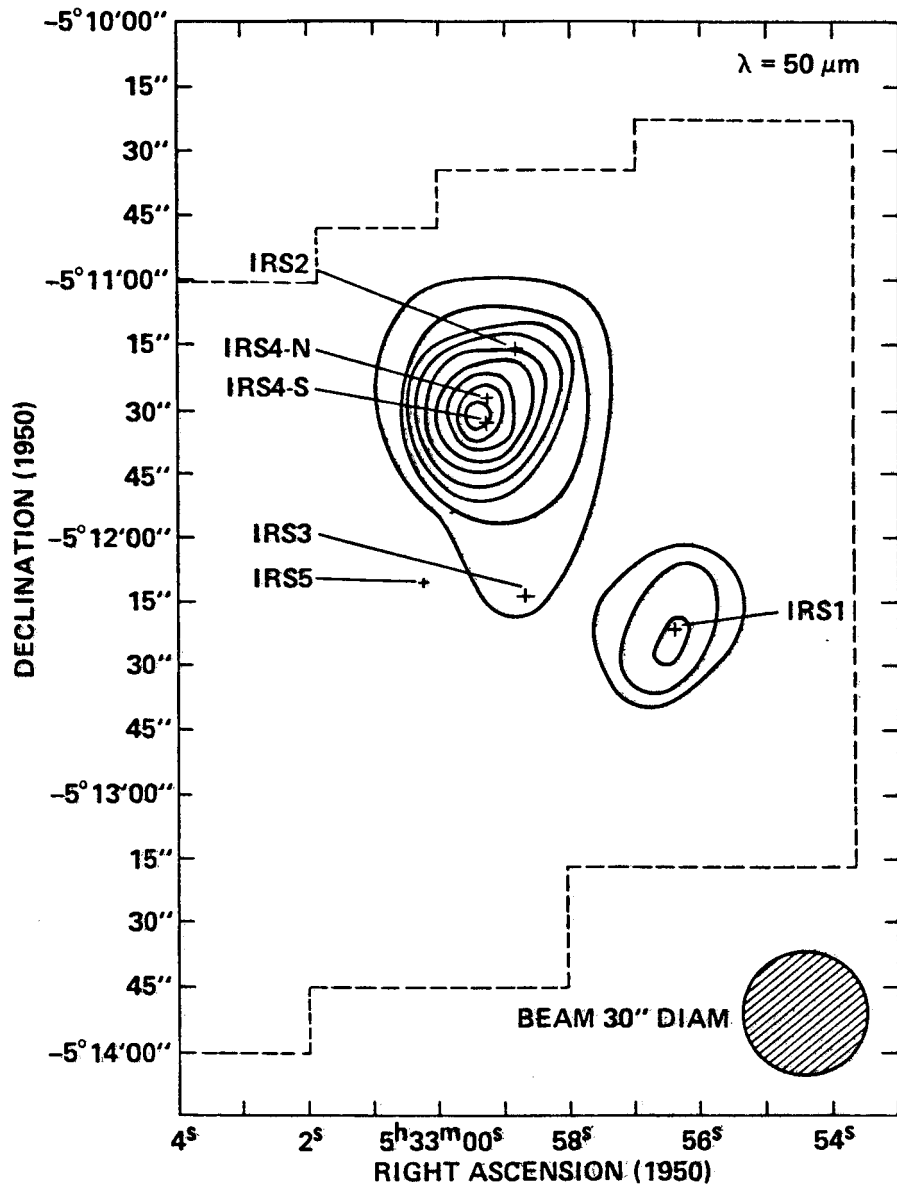


Fig. 1

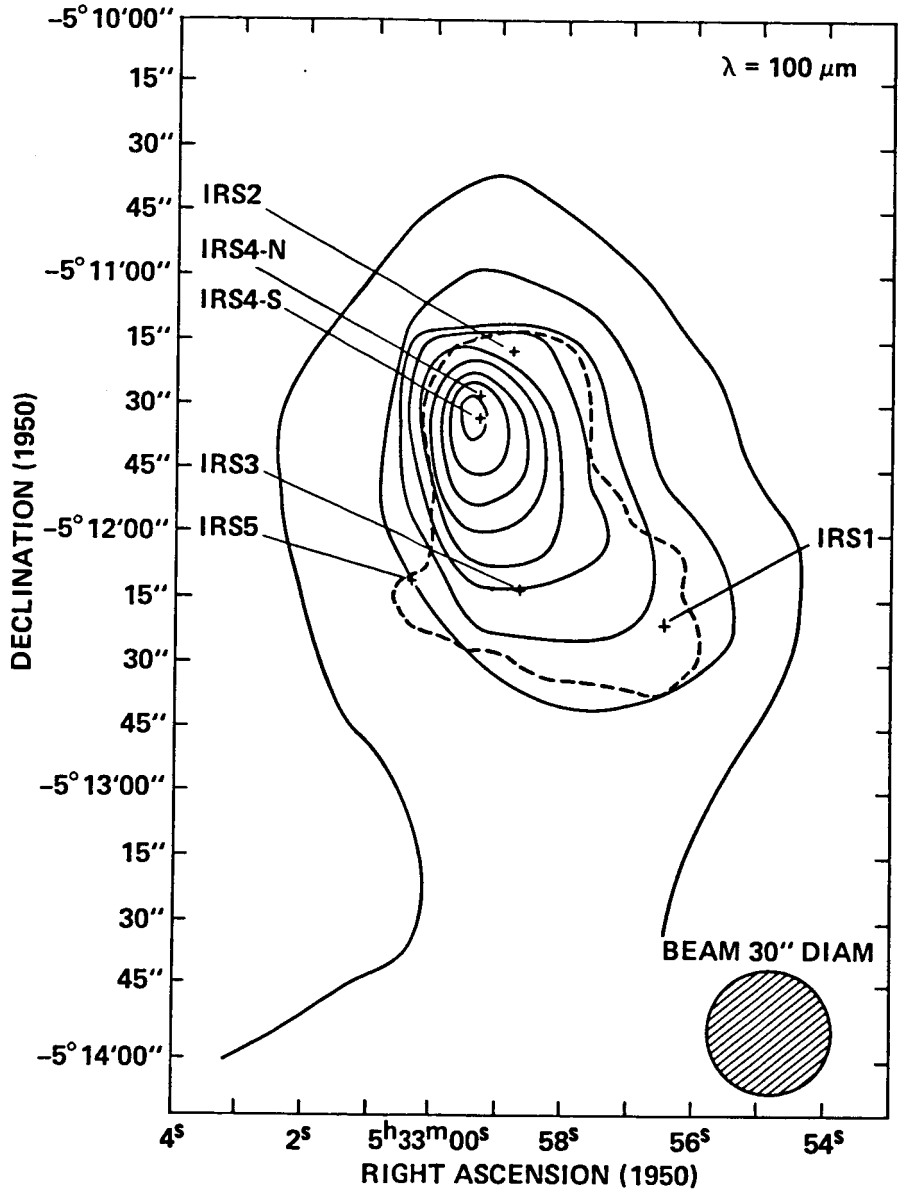


Fig. 2

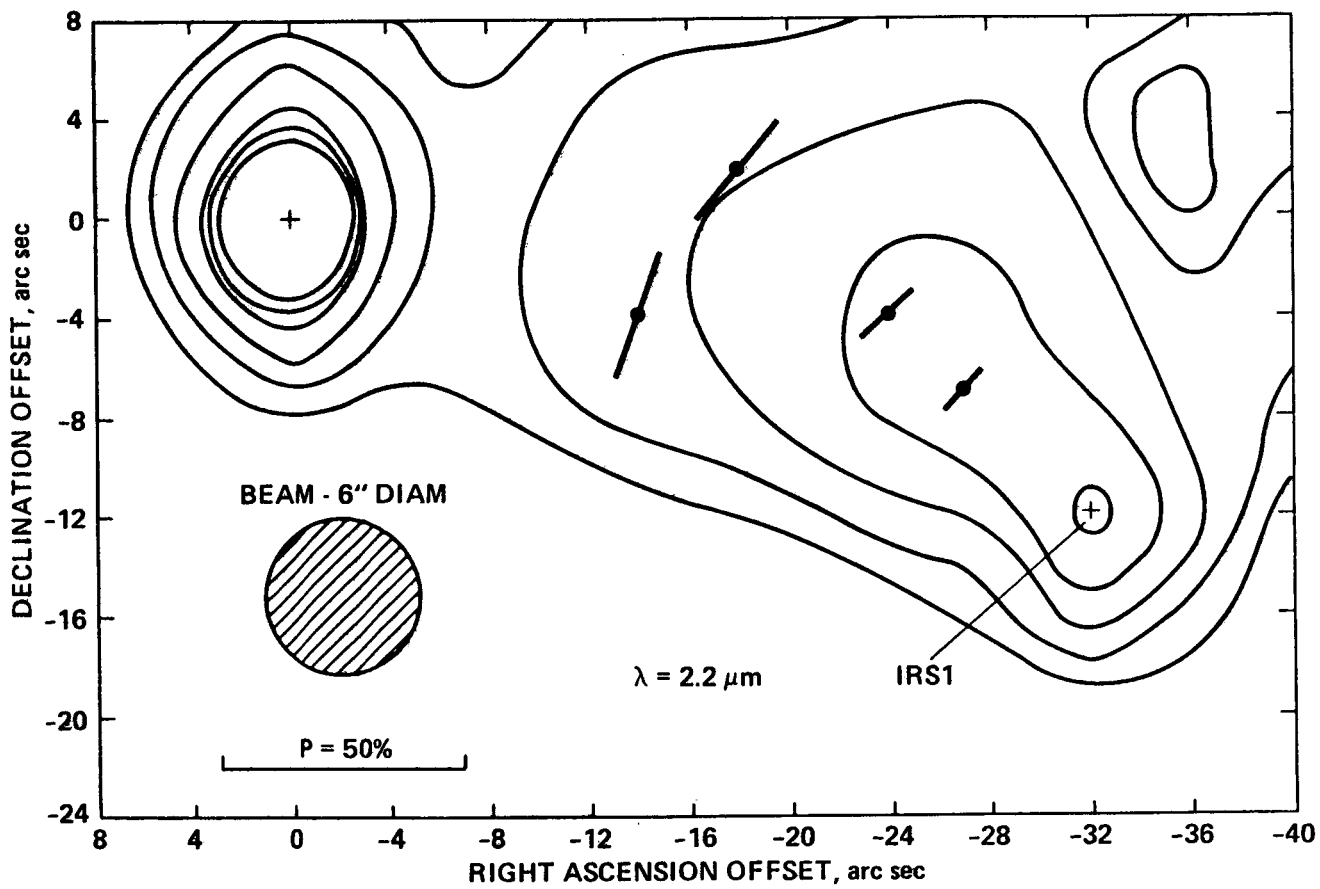


Fig. 3

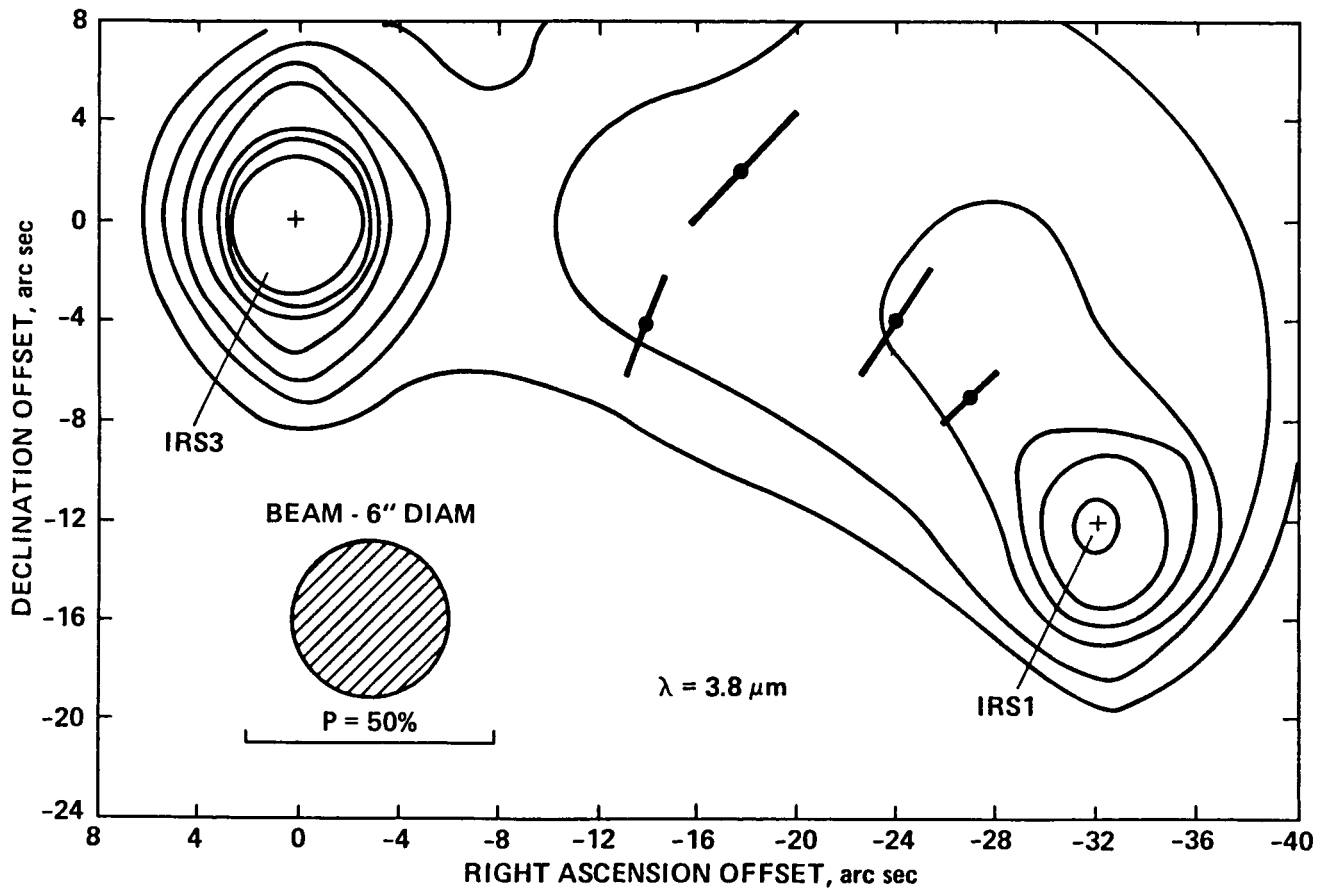


Fig. 4

Fig 5 (a)

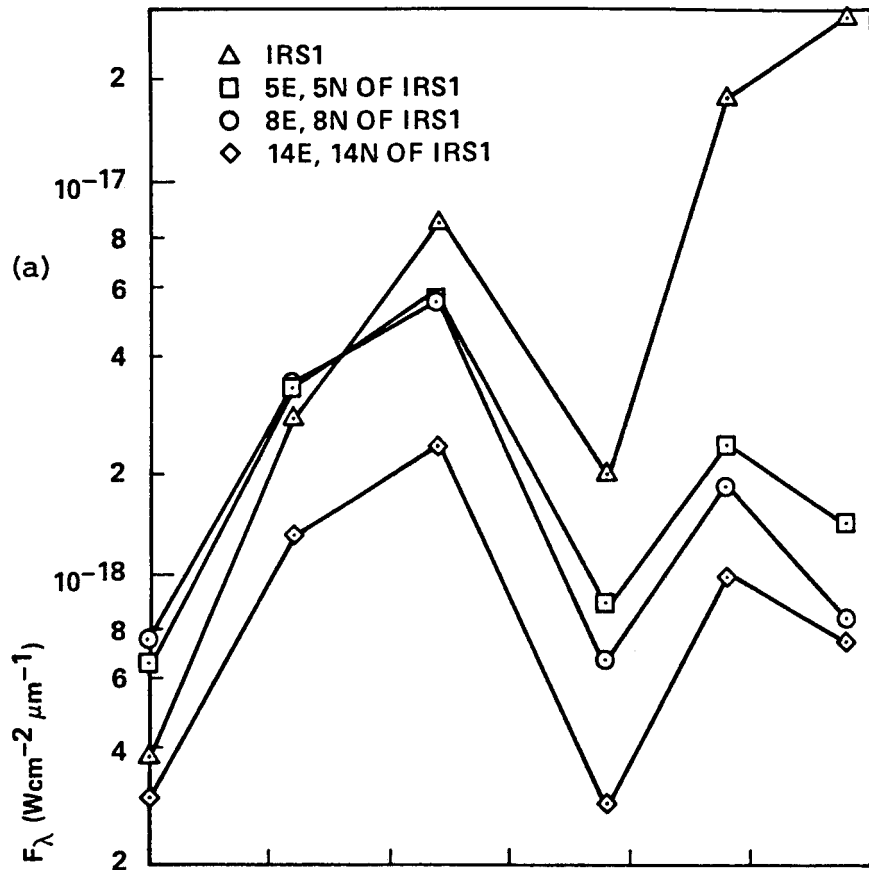


Fig 5 (b)

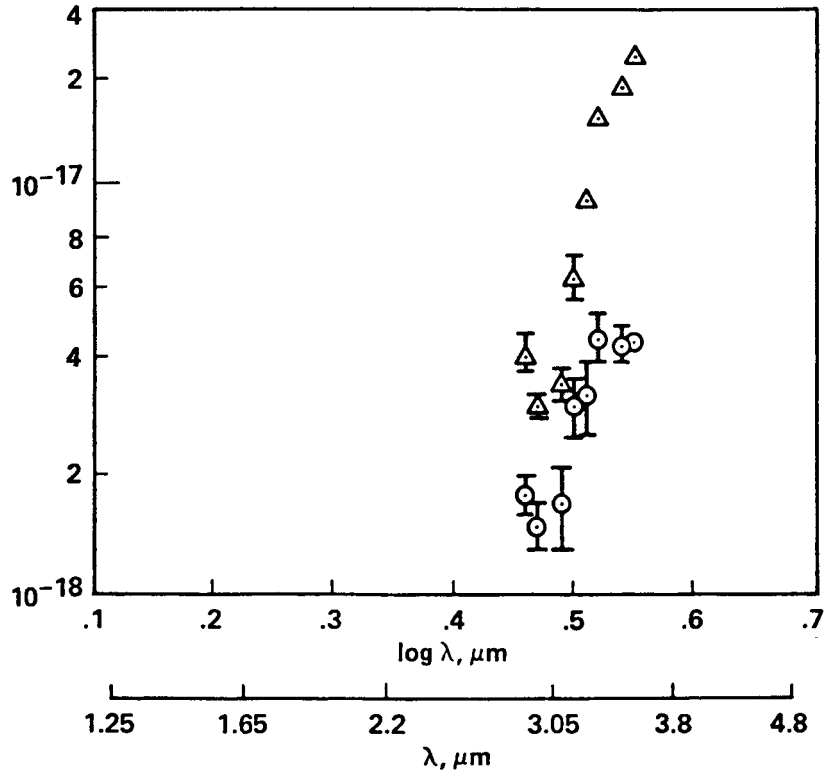


Fig. 5

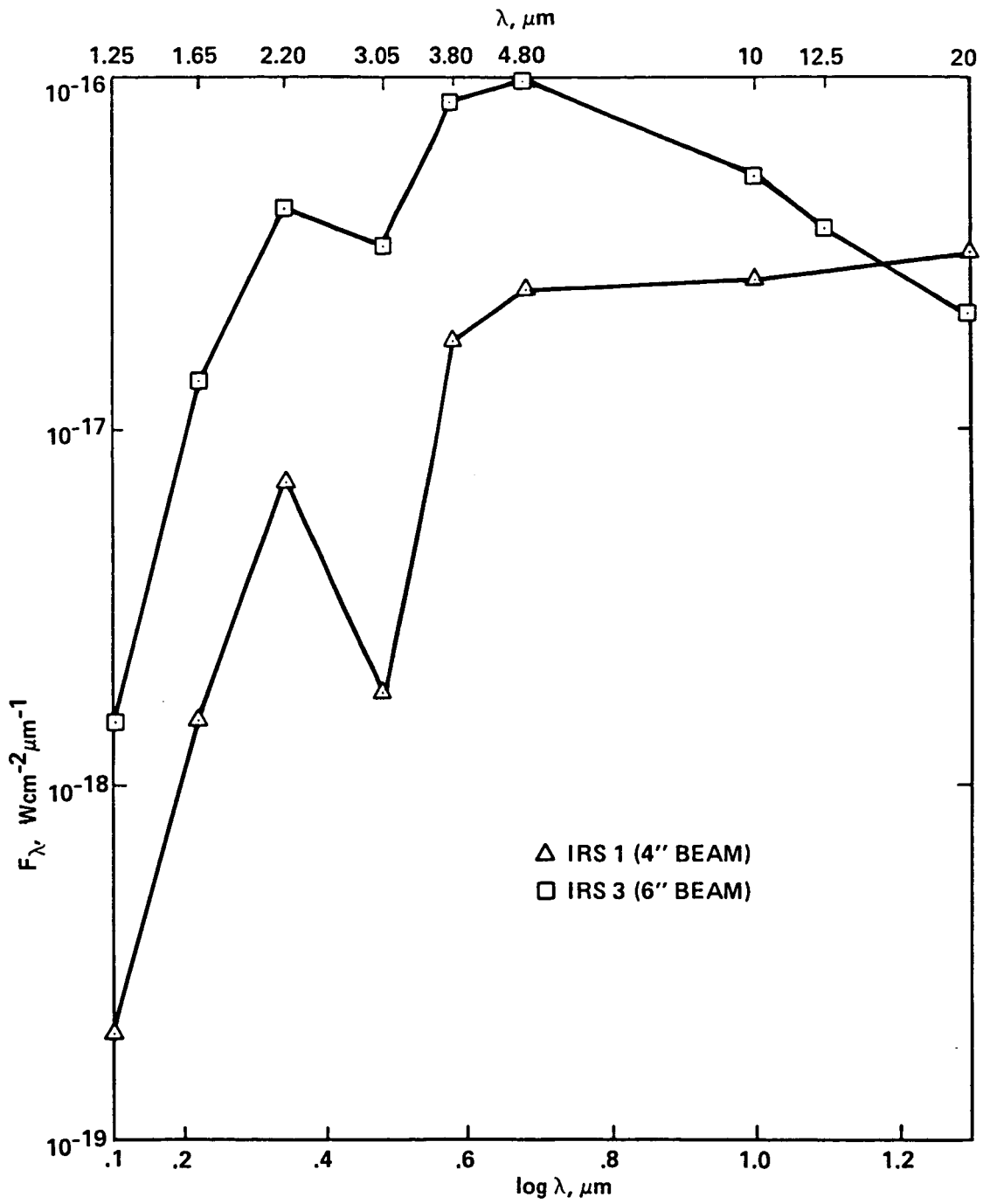


Fig. 6

OMC2 - IRS4 FLUX MAP AT 3.8 μm

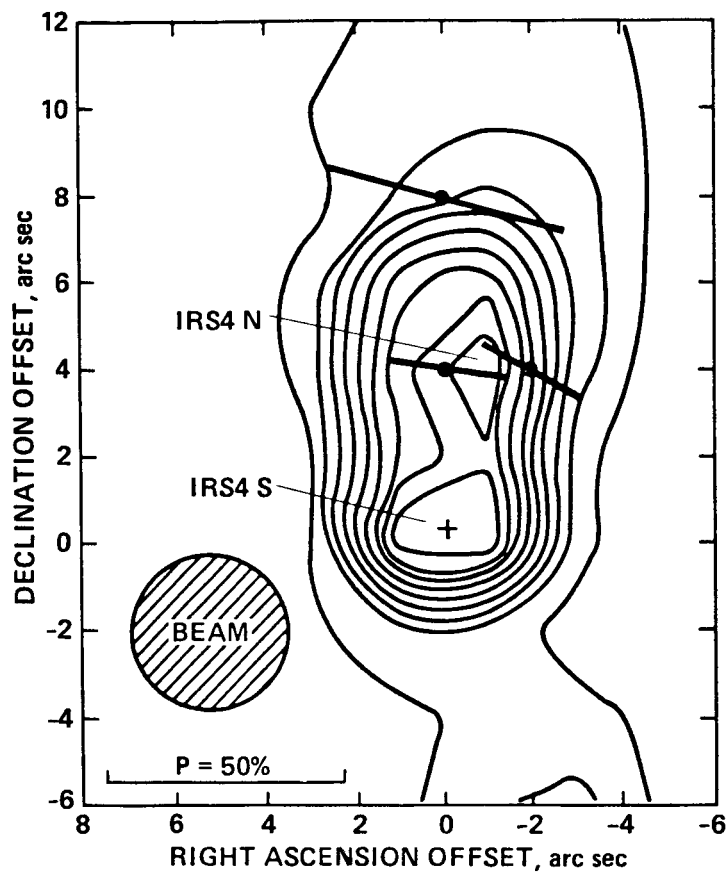


Fig. 7

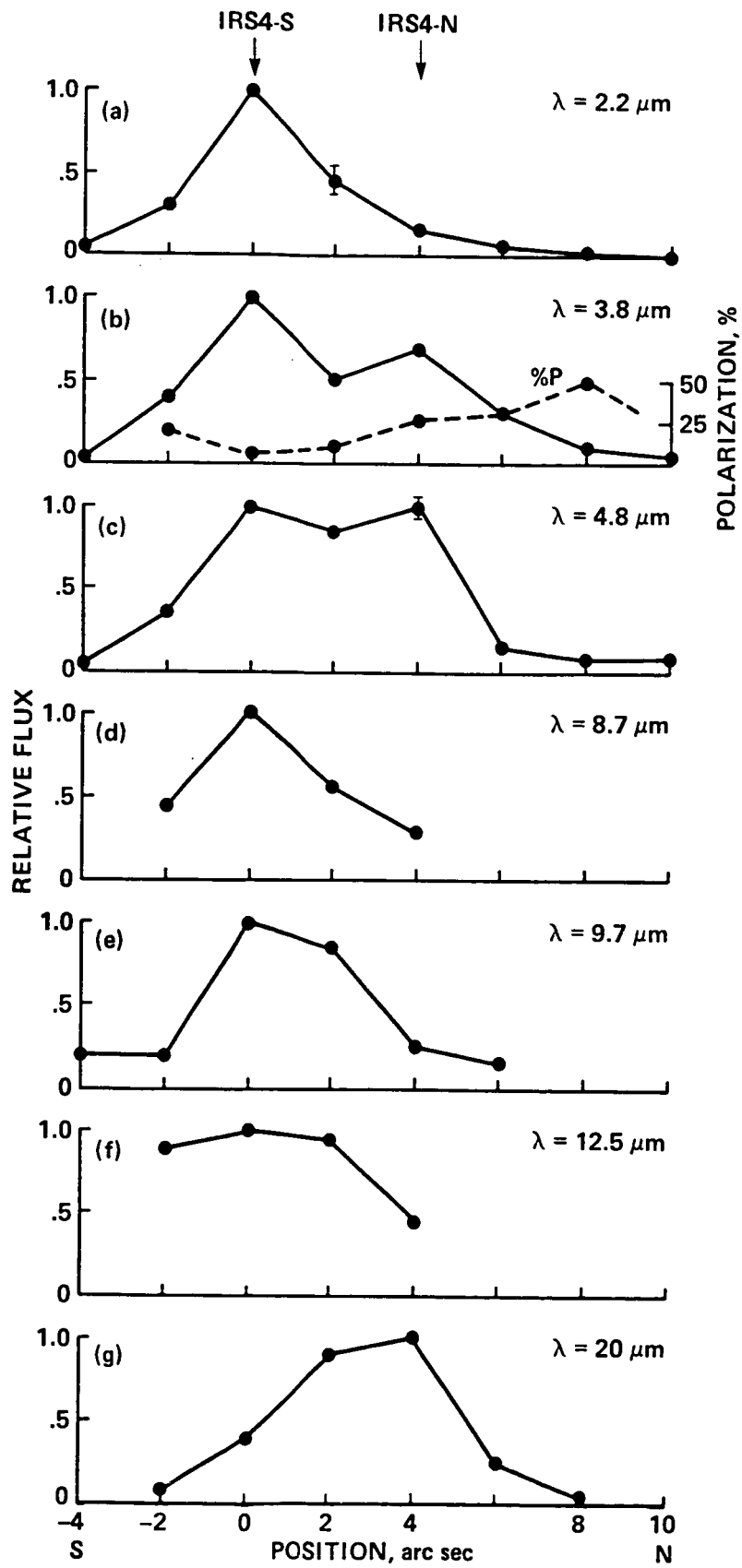


Fig. 8

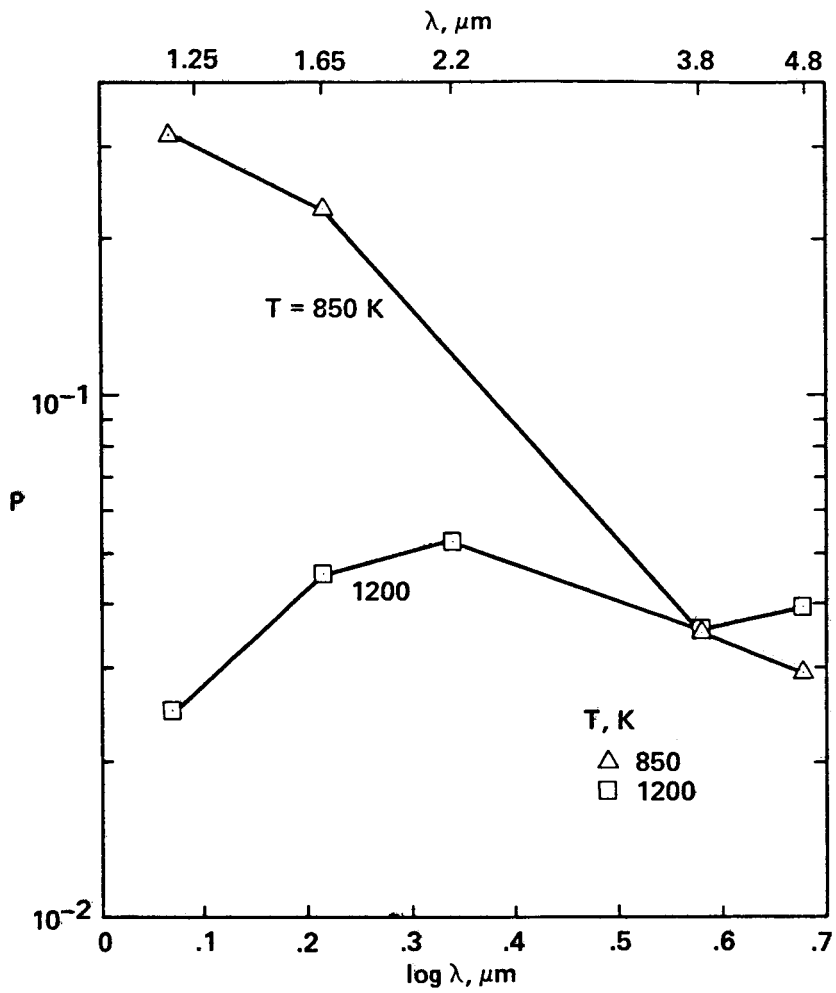


Fig. 9

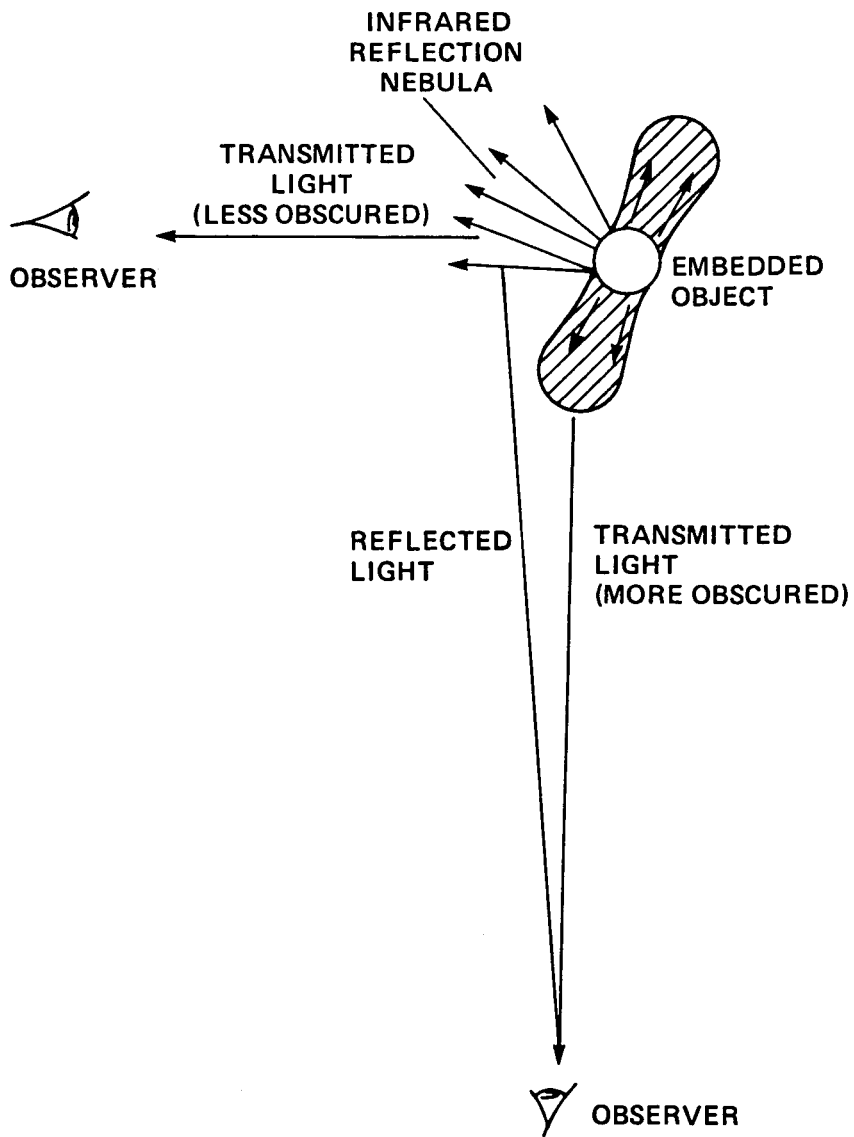


Fig. 10

Table 1

ORION MOLECULAR CLOUD 2 - SOURCE POSITIONS

Infrared Source	2.2 μ m Peak Flux Position		Offset from IRS3
	RA(1950) ± 0.1	DEC(1950) $\pm 1''$	
IRS 1	5 ^h 32 ^m 56 ^s .9	-5° 12' 21".3	33".3 West, 11".3 South
IRS 2	5 ^h 32 ^m 58 ^s .7	-5° 11' 18"	6" West, 52" North
IRS 3	5 ^h 32 ^m 59 ^s .1	-5° 12' 10" *	
IRS 4N	5 ^h 32 ^m 59 ^s .8	-5° 11' 26".1	9".7 East, 43".9 North
IRS 4S	5 ^h 32 ^m 59 ^s .8	-5° 11' 30".1	9".7 East, 39".9 North

* Gatley et al (1974)

TABLE 2. OBSERVATIONS

PHOTOMETRY	NEAR INFRARED PHOTOMETRY AND POLARIMETRY							FAR INFRARED PHOTOMETRY		
	IRS1 (4" BEAM)	IRS1 NEBULA (6" BEAM)			IRS4 (4" BEAM)		IRS3 (6" BEAM)	IRS2 (6" BEAM)	IRS1 (30" BEAM)	IRS4 (30" BEAM)
	a*	b*	c*	SOUTH	NORTH					
$\lambda, \mu\text{m}$	$F_{\lambda} (\times 10^{-18} \text{ Wcm}^{-2} \mu\text{m}^{-1})^{**}$							$F_{\lambda} (\times 10^{-18} \text{ Wcm}^{-2} \mu\text{m}^{-1})^{**}$		
1.25	0.2	0.7	0.8	0.3	1.6	0.1	1.5	0.1	20.0	60.0
1.65	1.5	3.4	3.5	1.4	7.1	0.3	13.8	0.7	15.0	50.0
2.2	7.1	5.6	5.6	2.4	10.4	1.4	41.8	2.3		
3.05	1.8	0.9	0.7	0.3	4.1	0.3	33.2	4.3		
3.8	17.8	2.4	2.0	1.1	6.8	5.0	86.2	11.9		
4.8	25.3	1.5	0.9	0.8	5.8	6.2	98.3	19.7		
8.7					3.5	1.0				
9.7					3.2	0.78±0.2				
10.3	26.0	< 0.4			3.4	1.2	51.4 (4" BEAM)			
12.5					3.1±0.4	1.4±0.4	37.0 (4" BEAM)			
20	30.0	< 0.7			3.3	9.4	21.0 (4" BEAM)			
30						21.0***				

POLARIMETRY	P(%)	$\theta(^{\circ})$	P(%)	$\theta(^{\circ})$	P(%)	$\theta(^{\circ})$	P(%)	$\theta(^{\circ})$	P(%)	$\theta(^{\circ})$
2.2	< 6	30	7	143	10	141	23	140	< 6	126
									19	89
3.8	< 6	139	13	139	25	149	31	137	< 6	62
									25	80
									< 6	114

* POINTS IN THE NEBULA LOCATED 5"E, 5"N (a), 8"E, 8"N (b) AND 14"E, 14"N (c) OF IRS1
 ** FLUX ERRORS ARE LESS THAN 10% UNLESS INDICATED; POLARIMETRY ERRORS ARE ± 2%; POSITION ANGLE UNCERTAINTIES ARE ± 3°; UPPER LIMITS ARE 3 σ
 *** WE ASSOCIATE THIS FLUX WITH THE POSITION OF IRS4-N

1. Report No. NASA TM 88259		2. Government Accession No.		3. Recipient's Catalog No.	
4. Title and Subtitle INFRARED REFLECTION NEBULAE IN ORION MOLECULAR CLOUD 2				5. Report Date June 1986	
				6. Performing Organization Code	
7. Author(s) Yvonne Pendleton,* M. W. Werner,* R. Capps,† and D. Lester‡				8. Performing Organization Report No. A-86276	
				10. Work Unit No.	
9. Performing Organization Name and Address *Ames Research Center, Moffett Field, CA 94035 †University of Hawaii, Honolulu, HI 96822 ‡University of Texas, Austin, TX 78712				11. Contract or Grant No.	
				13. Type of Report and Period Covered Technical Memorandum	
12. Sponsoring Agency Name and Address National Aeronautics and Space Administration Washington, DC 20546				14. Sponsoring Agency Code 352-02-03	
15. Supplementary Notes Preprint Series #53. Supported by NASA grants. Point of Contact: L. C. Haughney, Ames Research Center, MS 211-12, Moffett Field, CA 94035, (415)694-5339 or FTS 464-5339					
16. Abstract New observations of Orion Molecular Cloud-2 have been made from 1-100 μm using the NASA Infrared Telescope Facility and the Kuiper Airborne Observatory. An extensive program of polarimetry, photometry and spectrophotometry has shown that the extended emission regions associated with two of the previously known near infrared sources, IRS1 and IRS4, are infrared reflection nebulae, and that the compact sources IRS1 and IRS4 are the main luminosity sources in the cloud. The constraints from the far infrared observations and an analysis of the scattered light from the IRS1 nebula show that OMC-2/IRS1 can be characterized by $L \leq 500L_{\odot}$ and T-1000 K. The near infrared (1-5) μm albedo of the grains in the IRS1 nebula is greater than 0.08.					
17. Key Words (Suggested by Author(s)) Orion: Molecular Infrared: nebulae			18. Distribution Statement Unlimited Subject Category - 89		
19. Security Classif. (of this report) Unclassified		20. Security Classif. (of this page) Unclassified		21. No. of Pages 43	22. Price* A03